# Chronic use of pravastatin reduces insulin exocytosis and increases β-cell death in hypercholesterolemic mice

Estela Lorza-Gil[a], Alessandro G. Salerno[a], Amarylis C.B.A. Wanschel[a], Jean F. Vettorazzi[a], Mônica S. Ferreira[b], Thiago Rentz[a], Rodrigo R. Catharino[b], Helena C.F. Oliveira[a,*]

[a] Department of Structural and Functional Biology, Institute of Biology, State University of Campinas, Campinas, SP, Brazil
[b] Department of Clinical Pathology, Faculty of Medical Sciences, State University of Campinas, Campinas, SP, Brazil

A B S T R A C T

We have previously demonstrated that hypercholesterolemic LDL receptor knockout (LDLr$^{-/-}$) mice secrete less insulin than wild-type mice. Removing cholesterol from isolated islets using methyl-beta-cyclodextrin reversed this defect. In this study, we hypothesized that in vivo treatment of LDLr$^{-/-}$ mice with the HMGCoA reductase inhibitor pravastatin would improve glucose-stimulated insulin secretion. Female LDLr$^{-/-}$ mice were treated with pravastatin (400 mg/L) for 1–3 months. Isolated pancreatic islets were assayed for insulin secretion rates, intracellular calcium oscillations, cholesterol levels, NAD(P)H and SNARE protein levels, apoptosis indicators and lipidomic profile. Two months pravastatin treatment reduced cholesterol levels in plasma, liver and islets by 35%, 25% and 50%, respectively. Contrary to our hypothesis, pravastatin treatment increased fasting and fed plasma levels of glucose and decreased markedly (40%) fed plasma levels of insulin. In addition, ex vivo glucose stimulated insulin secretion was significantly reduced after two and three months (36–48%, $p < 0.05$) of pravastatin treatment. Although reducing insulin secretion and insulinemia, two months pravastatin treatment did not affect glucose tolerance because it improved global insulin sensitivity. Pravastatin induced islet dysfunction was associated with marked reductions of exocytosis-related SNARE proteins (SNAP25, Syntaxin 1A, VAMP2) and increased apoptosis markers (Bax/Bcl2 protein ratio, cleaved caspase-3 and lower NAD(P)H production rates) observed in pancreatic islets from treated mice. In addition, several oxidized phospholipids, tri- and diacylglycerols and the proapoptotic lipid molecule ceramide were identified as markers of pravastatin-treated islets. Cell death and oxidative stress ($H_2O_2$ production) were confirmed in insulin secreting INS-1E cells treated with pravastatin. These results indicate that chronic treatment with pravastatin impairs the insulin exocytosis machinery and increases β-cell death. These findings suggest that prolonged use of statins may have a diabetogenic effect.

© 2016 Elsevier Ireland Ltd. All rights reserved.

## 1. Introduction

Type 2 diabetes mellitus (T2D) is related to both insulin resistance in target tissues and pancreatic islet malfunction and failure (Halban et al., 2014). Progression from the insulin-resistant state to T2D occurs in a subset of individuals in whom β-cells are unable to maintain increased insulin secretion upon a chronic demand. In these cases, β-cells become exhausted and dysfunctional with reduced secretory response to glucose stimulus,

reduced insulin synthesis and eventually β-cell apoptosis. The reasons why β-cells become dysfunctional in some individuals whereas others remain in an insulin resistant state for prolonged periods are not well understood. Several hypotheses including glucotoxicity (Gleason et al., 2000) and lipotoxicity (Unger, 1995) caused by chronic hyperglycemia and chronic hyperlipidemia, respectively, have been raised. It has been suggested that the lipotoxicity associated with increased free fatty acid accumulation in β-cells, as occurs in obesity, can cause β-cell death (Poitout and Robertson, 2008).

Previous in vitro studies have indicated that cholesterol may also play a major role in controlling β cell function (Vikman et al., 2009). In vivo studies also demonstrated that cholesterol accumulation in β-cells is associated with reduced insulin secretion, β-cell dysfunction and decreased β-cell mass in genetic

* Corresponding author at: Lipid Metabolism Laboratory, Department of Structural and Functional Biology, Institute of Biology, State University of Campinas, Rua Monteiro Lobato, 255 Campinas, SP CEP 13083-862, Brazil.
    E-mail address: ho98@unicamp.br (H.C.F. Oliveira).

modified mouse models such as the β-cell-specific ABCA1 knockout and SREBP-2 transgenic (Brunham et al., 2007; Fryirs et al., 2009; Hao et al., 2007; Ishikawa et al., 2008). In pancreatic β-cell membranes, cholesterol and sphingolipids form lipid raft domains that are important to anchor membrane proteins involved in the secretory process such as the voltage-gated calcium channel $Ca_v2.1$ (Chamberlain et al., 2001; Taverna et al., 2004) and the SNARE proteins (soluble N-ethylmaleimide sensitive factor attachment receptor) (Taverna et al., 2004; Wiser et al., 1999) that drive insulin vesicle fusion with the plasma membrane (Bruns and Jahn, 2002; Hanson et al., 1997).

We previously demonstrated that hypercholesterolemic LDL receptor knockout mice ($LDLr^{-/-}$) exhibited impaired insulin secretion due to lower glucose uptake and metabolism, reduced $PKA\alpha$ and SNARE proteins expression and calcium handling deficiency. These disturbances were reversed by removing cholesterol from isolated islets in vitro with methyl beta cyclodextrin. (Bonfleur et al., 2010, 2011; Souza et al., 2013). Therefore, we proposed that primary (genetic) hypercholesterolemia increases the risk of diabetes development. Here, we hypothesized that treating these hypercholesterolemic mice with inhibitors of the 3-hydroxy-3-methyl-glutaryl coenzyme A reductase (HMGCoA red) would decrease islet cholesterol content and recover the insulin secretory capacity of $LDLr^{-/-}$ mice. Statins have been used to treat hypercholesterolemic patients for cardiovascular disease prevention since the late 80s (Taylor et al., 2013). These drugs are first-line agents that effectively reduce LDL-cholesterol. Other beneficial pleiotropic effects of statins have been reported such as improvements in endothelial function and stabilization of atherosclerotic plaques as well as anti-inflammatory and antioxidant actions (Davignon et al., 2004). However, adverse effects have also been identified since statins have been available, and two of the most common clinician concerns are myopathy and diabetes (Desai et al., 2014).

## 2. Materials and methods

### 2.1. Animals

Low-density lipoprotein receptor knockout ($LDLr^{-/-}$) female mice on the C57BL/6J background, originally from the Jackson Laboratory (Bar Harbor, ME), were obtained from the breeding colony of the State University of Campinas (UNICAMP). Animal experiments were approved by the University's Committee for Ethics in Animal Experimentation (CEUA/UNICAMP, protocol # 3001–1). The mice had free access to regular rodent AIN93-M diet (14% protein) and water and were housed at $22 \pm 1\,°C$ on a 12 h light/dark cycle. Female mice (4 weeks old) were treated with pravastatin for 4–12 weeks dissolved in the drinking water (400 mg/L). The estimated pravastatin sodium (Medley) dose of 40 mg/kg body weight per day was based on the drink consumption rate measurements (3.6 mL/day). Controls received filtered tap water without pravastatin. Additional groups of wild type mice (C57BL6/J) were also treated with pravastatin.

### 2.2. Plasma biochemical analyses

Blood glucose was measured using a glucose analyzer (Accu-Chek Advantage; Roche Diagnostics, Basel, Switzerland), and plasma cholesterol, triglycerides and free fatty acids were measured using standard commercial kits (Roche Diagnostics GMBH, Mannheim, Germany; Wako Chemical, Neuss, Germany) according to the manufacturer's instructions. Blood samples were obtained between 8 and 9:00 am after a 12 h fasting period (food was removed at 8:00 pm).

### 2.3. Oral glucose tolerance test (OGTT) and insulin tolerance test (ITT)

After 12 h of fasting (food removed at 8:00 pm and blood obtained between 8 and 9:00 am), mice received an oral dose of glucose solution (1.5 g/kg body weight). Basal blood samples were collected from the tail tip before ($t = 0$ min) and 15, 30, 60, 90 and 120 min after glucose ingestion. For the ITT, blood was taken from mice that had been fasted for 3 h before ($t = 0$ min) and 5, 10, 15, 30 and 60 min after an i.p. insulin injection (0.75 U/kg body weight, regular human insulin, Eli Lilly Co.) for glucose analysis.

### 2.4. Pancreatic islet isolation and static insulin secretion

Pancreatic islets were isolated from fasted mice by collagenase type V (0.8 mg/mL; Sigma) digestion and were then selected with a microscope (Boschero and Delattre, 1985). Four replicates of four islets/well in each condition (basal and glucose stimulated) from each mouse ($n = 4$–8 mice per group) were used for the insulin secretion assay. Islets were pre-incubated for 30 min at $37\,°C$ in Krebs-bicarbonate buffer (KBB) of the following composition: 115 mmol/L NaCl, 5 mmol/L KCl, 2.56 mmol/L $CaCl_2$, 1 mmol/L $MgCl_2$, 10 mmol/L $NaHCO_3$, 15 mmol/L HEPES, supplemented with 5.6 mmol/L glucose and 0.3% BSA, equilibrated with a mixture of 95% $O_2$/5% $CO_2$, pH 7.4. The islets were further incubated during 1 h in KBB containing glucose (2.8 or 11.1 mmol/L). At the end of the incubation period, media insulin content was measured by radioimmunoassay (Scott et al., 1981).

### 2.5. Cytoplasmatic $Ca^{+2}$ and NADPH response to glucose

For intracellular calcium recordings, islets were incubated with fura-2 acetoxymethyl ester (5 μM) for 1 h at $37\,°C$ in KBB buffer that contained 5.6 mM glucose, 0.3% BSA and pH 7.4. $Ca^{+2}$ recordings in whole islets (8 fields per islet, six islets per mouse, 7 mice per group) were obtained by imaging intracellular $Ca^{+2}$ using an inverted epifluorescence microscope (Nikon UK, Kingston, UK), a digital camera (Hamamatsu Photonics, Barcelona, Spain) and a dual-filter wheel (Sutter Instrument Co., Navato, CA) that was equipped with 340 and 380 nm filters, 10 nm band-pass, as previously described (Rafacho et al., 2010). Fluorescence recordings were expressed as the ratio of fluorescence at 340 and 380 nm (F340/F380). NAD(P)H auto-fluorescence was monitored using the imaging system described above. NAD(P)H auto-fluorescence was excited with a 365 nm filter, whereas emission was filtered at $445 \pm 25$ nm, as previously described (Rafacho et al., 2010). Six fields per islet, 6 islets/mouse, 5 mice per group.

### 2.6. Western blotting

Islets (150–200 per mouse) were homogenized in urea lysis buffer and treated with Laemmli loading buffer containing dithiothreitol. After heating to $95\,°C$ for 5 min, the proteins were separated by electrophoresis (40 μg protein/lane, 12% or 10% gels) and were then transferred to nitrocellulose membranes. The nitrocellulose membranes were treated for 1.5 h with a blocking buffer (5% BSA, 10 mmol/L tris, 150 mmol/L NaCl, and 0.02% Tween 20) and were subsequently incubated with the following primary antibodies: Caspase-3 (Millipore), BAX (Cell signaling), Bcl-2 (Cell signaling), SNAP25 (Sigma), VAMP-2 (Calbiochem), Syntaxin-1A (Santa Cruz Biotechnology), IDE (Abcam), HMGCoA red (Millipore). Rabbit polyclonal antibody against GAPDH (Santa Cruz Biotechnology) was used as an internal control. Membranes were then incubated with anti-mouse or anti-rabbit horseradish peroxidase-conjugated secondary antibodies (1:10000, Invitrogen). Detection was performed using enhanced chemiluminescence (SuperSignal

West Pico, Pierce, Rockford, IL). Band intensities were quantified by optical densitometry (Scion Image, Frederick, MD).

### 2.7. DNA fragmentation detection by terminal deoxynucleotidyl transferase mediated-dUTP nick end labeling (TUNEL)

Islets (80–100 per mice) were incubated for 24 h in labtek slides (Thermo Scientific) and fixed with 4% paraformaldehyde in PBS 30 min. Slides were then washed with PBS and permeabilized by adding 0.05% Triton X-100 for 15 min. Endogenous peroxidase activity was blocked with 3% hydrogen peroxide in methanol for 30 min and assayed for DNA fragmentation using a TUNEL assay kit (In Situ Cell Death Detection Kit, POD-Roche Mannheim, Germany) according to the manufacturer's instructions. Islets were then incubated with insulin-specific primary antibodies (Dako) for 2 h and with TRITC-labeled secondary antibodies (Sigma) for 2 h. Islets were mounted with Vectashield medium with DAPI and were visualized. Four islets (replicates) from each mouse were randomly selected at $63\times$ magnification and positive apoptotic cells were counted. Results are mean of 3 mice per group. Observations and photomicrographs were performed with a Zeiss LSM780-NLO (Carl Zeiss AG, Germany) confocal microscope.

### 2.8. Immunofluorescence

Serial frozen sections of 4% paraformaldehyde fixed pancreas were prepared from OCT embedded tissue using a cryostat. Sections were blocked with 5% BSA in PBS for 1 h. Sections were then incubated with primary antibodies that were specific for VAMP-2 or Syntaxin-1 overnight followed by 2 h incubation with Alexa Fluor (Life technologies) secondary antibodies. Next, sections were incubated for 2 h with insulin primary antibody (Dako) and then with TRITC (Sigma) secondary antibody for 2 h. Sections were mounted with Vectashield medium with DAPI. Pictures were taken on Zeiss LSM780-NLO (Carl Zeiss AG, Germany) confocal microscope and analyzed with ImageJ software.

### 2.9. Lipidomic analyses by MALDI-Mass Spectrometry Imaging (MSI)

Pancreatic islets were washed with milliQ $H_2O$ and deposited in a glass plate. Matrix coating was performed using a commercial airbrush that sprayed α-cyano-4-hydroxycinnamic acid (Sigma–Aldrich, PA, USA) (10 mg/mL in 1:1 acetonitrile/methanol solution). Images and mass spectra were acquired using a MALDI LTQ-XL instrument that was equipped with imaging features (Thermo Scientific, CA, USA). The instrument has an ultraviolet laser as ionization source and a quadrupole ion trap analyzing system. All of the data were acquired in the negative ion mode at 4 µJ laser energy and in the m/z range of 600 to 1000. For image acquisition, a 30 µm raster width was selected. Fragmentation data (MS/MS) were acquired by setting the collision-induced energy to 40 eV. Helium was used as the collision gas. Each ion was fragmented in triplicate. All of the imaging data were then processed using ImageQuest software v.1.0.1 (Thermo Scientific, CA, USA). Statistical analysis and chemical marker identification were performed by Principal Component Analysis (PCA) using Unscrambler v.9.7 (CAMO Software, Trondheim, Norway). The software clustered samples according to the relationship between $m/z$ and intensity, and the results were expressed as groups of samples with the same characteristics when these parameters were considered. MS/MS reactions were performed with each potential chemical marker identified by PCA. The lipid MAPS online database (University of California, San Diego, CA, USA— www.lipidmaps.org) and METLIN (Scripps Center for Metabolomics, La Jolla, CA, USA) were consulted to guide the choice for potential lipid markers. Their structures were later input into Mass Frontier software v.6.0 (Thermo Scientific, CA, USA), where a number of fragments and mechanisms were modeled. Mass Frontier uses literature data and mathematical calculations to propose fragmentation mechanisms and products (Urayama et al., 2010). Structures were assigned to molecules that presented the highest number of matches between MS/MS experimental data and Mass Frontier fragments.

### 2.10. Islet cholesterol content by MALDI-MSI

For relative quantification, cholesterol standard (Sigma–Aldrich ≥ 99%) and both control and pravastatin-treated pancreatic islets were submitted to MS/MS analysis for $m/z$ 369 in positive ion mode. All of the images generated by MALDI-MSI were extracted on gray scale to relative quantification using ImageJ (National Institutes of Health, USA—Open Source). The area was standardized in number of pixels and the ImageJ software assigned a value for the selection based on the intensity of each sample.

### 2.11. INS-1E cell culture

INS-1E cells (kindly provided by C. Wollheim, Centre Medical Universitaire, Geneva, Switzerland) were cultured in a humidified atmosphere containing 5% $CO_2$ and maintained in RPMI 1640 medium [11 mM glucose, 5% FBS, 1% 4-(2-hydroxyethyl)-1-piperazineethanesulfonic acid (HEPES), 1% sodium pyruvate, and 1% penicillin/streptomycin] until 60–80% confluence. After this period, the cells were incubated with pravastatin sodium salt

**Table 1**
Body weight (g) and plasma concentrations of lipids in untreated (control) and pravastatin treated LDLr$^{-/-}$ mice.

|  | Treatment period | 1 month | 2 months | 3 months |
|---|---|---|---|---|
| Body weight (g) | Control | 16.1 ± 0.6 (10) | 19.7 ± 0.3 (16) | 19.9 ± 0.3 (6) |
|  | Pravastatin | 15.9 ± 1.2 (10) | 19.2 ± 0.2 (16) | 19.4 ± 0.2 (6) |
| FFA (mmol/L) | Control | 1.4 ± 0.0 (3) | 1.2 ± 0.1 (5) | 1.2 ± 0.1 (7) |
|  | Pravastatin | 1.4 ± 0.1 (3) | 1.0 ± 0.0 (6) | 1.4 ± 0.1 (7) |
| TG (mg/dL) | Control | 189.2 ± 52.8 (3) | 114.7 ± 13.5 (5) | 208.9 ± 33.5 (8) |
|  | Pravastatin | 198.2 ± 3.2 (3) | 106.5 ± 17.9 (6) | 151.8 ± 16.4 (8) |
| CHOL (mg/dL) | Control | 359.8 ± 11.9 (10) | 524.8 ± 25.2 (14) | 564.9 ± 33.0 (14) |
|  | Pravastatin | 235.7 ± 5.8 (10)[*] | 341.7 ± 16.3 (15)[*] | 368.3 ± 23.0 (14)[*] |

FFA: free fatty acids, TG: triglycerides, CHOL: cholesterol. Mean ± SE ($n$).
[*] $p < 0.001$ vs. control, Student $t$ test. Pravastatin 400 mg/L drinking water.

(Sigma) 1–50 µM for 12–48 h. Subsequently, cells were used for $H_2O_2$ measurements and for Western blot analyses.

### 2.12. INS-1E cell $H_2O_2$ production

$H_2O_2$ release was monitored by measuring the conversion of Amplex Red to highly fluorescent resorufin in the presence of added horseradish peroxidase. $0.5 \cdot 10^5$ cells were incubated in 96-well cell culture plates with pravastatin sodium salt (Sigma) 1–50 µM for 12–48 h. On the day of the experiment, cells were incubated in a mixture contained 50 µM Amplex Red reagent (Invitrogen) and 0.1 U/mL horseradish peroxidase in Krebs–Ringer phosphate buffer (145 mM NaCl, 5.7 mM sodium phosphate, 4.86 mM KCl, 0.54 mM $CaCl_2$, 1.22 mM $MgSO_4$, 11.1 mM glucose, pH 7.35). This assay was conducted in the presence and absence of catalase (500 U/mL) for 1 h. Fluorescence was monitored over time with a temperature-controlled SpectraMax I3 Microplate Reader (Molecular Devices) using excitation and emission wavelengths of 560 and 590 nm, respectively.

### 2.13. Statistical analysis

The data are presented as the mean ± standard error (SE) ($n$ is indicated in each figure). The groups were compared using an unpaired Student's $t$ test. The level of significance was set at $P \leq 0.05$.

## 3. Results

Plasma lipid concentrations in untreated (control) and pravastatin-treated $LDLr^{-/-}$ mice are demonstrated in Table 1. As expected, pravastatin treatment resulted in a reduction of total cholesterol levels compared with untreated control mice. Pravastatin treatment for 1–3 months reduced total plasma cholesterol levels by 35%. No differences were observed in plasma free fatty acid and triglyceride levels of treated $LDLr^{-/-}$ mice (Table 1). In addition to the hypocholesterolemic effect, pravastatin treatment reduced hepatic cholesterol content after one and two months of treatment by 20–25% ($2.55 \pm 0.17$ vs. $1.94 \pm 0.10$ and $2.32 \pm 0.14$ vs. $1.88 \pm 0.11$ µg/mg protein for untreated vs. one- and two-month treated mice, respectively, $p = 0.02$). Hepatic HMGCoA reductase protein expression was not altered by pravastatin treatment (Supplementary Fig. 1). No differences were observed in hepatic triglyceride content (data not shown). Wild type mice treated with pravastatin during 2 months had no changes in their plasma cholesterol concentrations (Supplementary Table 1).

### 3.1. Effects of pravastatin on glucose homeostasis in $LDLr^{-/-}$ mice

Pravastatin treatment for 2 months increased fasting (11%) and fed (25%) plasma levels of glucose but did not alter fasting insulin and the index of insulin resistance HOMA-IR (Table 2). However, in the fed state, pravastatin caused a marked decrease in insulin (42%) levels, so that the ratio glucose/insulin was 1.6 fold increased in the treated mice (Table 2). On the contrary, wild type mice treated with pravastatin during 2 months had no changes in their plasma levels of glucose and insulin in both states (Supplementary Table 1).

In order to further investigate glucose homeostasis in $LDLr^{-/-}$ mice, we analyzed their glucose tolerance (GTT) and insulin sensitivity (ITT) (Fig. 1). Pravastatin treatment for 2 months did not affect glucose tolerance (Fig. 1A). Only time zero (fasting state) glucose levels were increased in pravastatin treated mice. Glucose tolerance was not disturbed also after 3 months of pravastatin treatment (data not shown). Plasma insulin levels during GTT (area under the curve) were significantly decreased by 31% in the pravastatin group (Fig. 1B), what is in agreement with the fed insulin plasma levels (Table 2). Lower insulin plasma levels are not due to increased liver degradation because insulin degrading enzyme (IDE) expression did not change with pravastatin treatment (Supplementary Fig. 1). Since the glucose tolerance is unaffected under lower insulin levels we checked the $LDLr^{-/-}$ mice insulin sensitivity by ITT. Fig. 1C shows that 2 months pravastatin treatment increased insulin sensitivity, as demonstrated by a 40% higher initial (0–10 min) glucose disappearance rate (Kitt) after insulin administration, which can explains the preserved glucose tolerance under lower insulin levels. Thus, lower insulin levels may represent a deficit of β-cell function in pravastatin-treated mice.

### 3.2. Pravastatin disturbed insulin secretion in isolated islets from $LDLr^{-/-}$ mice

Pravastatin-treated $LDLr^{-/-}$ mice displayed a time-dependent inhibition of insulin secretion under glucose-stimulated (11.1 mM glucose) conditions (Fig. 2A–C). Treatment for 1 month did not affect insulin secretion; however, significant reductions in insulin secretion were observed after 2 (36% $p < 0.05$) and 3 months (48% $p < 0.05$) of pravastatin treatment. The observed effect was not due to reductions in total islet insulin content (Fig. 2D). Notably, pravastatin treatment reduced cholesterol content in $LDLr^{-/-}$ mouse islets by 50% ($p = 0.039$) compared with non-treated mice (Fig. 2E, Supplementary Fig. 2).

From now on, we decided to further investigate the possible statin islet toxic mechanisms only after 2-month treatment, when we first observed the statin detrimental effects.

### 3.3. Two month pravastatin treatment reduced SNARE protein expression in isolated $LDLr^{-/-}$ mouse islets

Insulin granule exocytosis is a multiple-step process that depends on the elevation of intracellular $[Ca^{+2}]$ as well as the activity of different membrane proteins that constitute the secretory apparatus, named SNARE proteins. Both calcium

**Table 2**
Plasma glucose and insulin levels, water consumption and body weight in $LDLr^{-/-}$ mice untreated (control) and treated with pravastatin during two months.

| | Fasted | | Fed | |
|---|---|---|---|---|
| | Control | Pravastatin | Control | Pravastatin |
| Glucose (mg/dL) | $87.8 \pm 2.7$ | $97.8 \pm 3.8^*$ | $136.9 \pm 5.0$ | $171.1 \pm 8.4^*$ |
| Insulin (ng/mL) | $0.45 \pm 0.08$ | $0.48 \pm 0.05$ | $0.81 \pm 0.12$ | $0.47 \pm 0.10^*$ |
| Glucose/insulin | $258.2 \pm 63.2$ | $193.1 \pm 23.0$ | $199.5 \pm 28.7$ | $326.9 \pm 50.8^*$ |
| HOMA-IR | $2.75 \pm 0.56$ | $2.96 \pm 0.34$ | x | x |
| Water consumption (mL/day) | x | x | $3.60 \pm 0.08$ | $3.62 \pm 0.12$ |
| Body weight (g) | $19.7 \pm 0.3$ | $19.2 \pm 0.2$ | x | x |

Mean ± SE ($n = 16$ for fasted glucose and body weight, and $n = 8$ for others). Homa-IR: insulin resistance index (homeostatic model assessment). Pravastatin 400 mg/L drinking water.
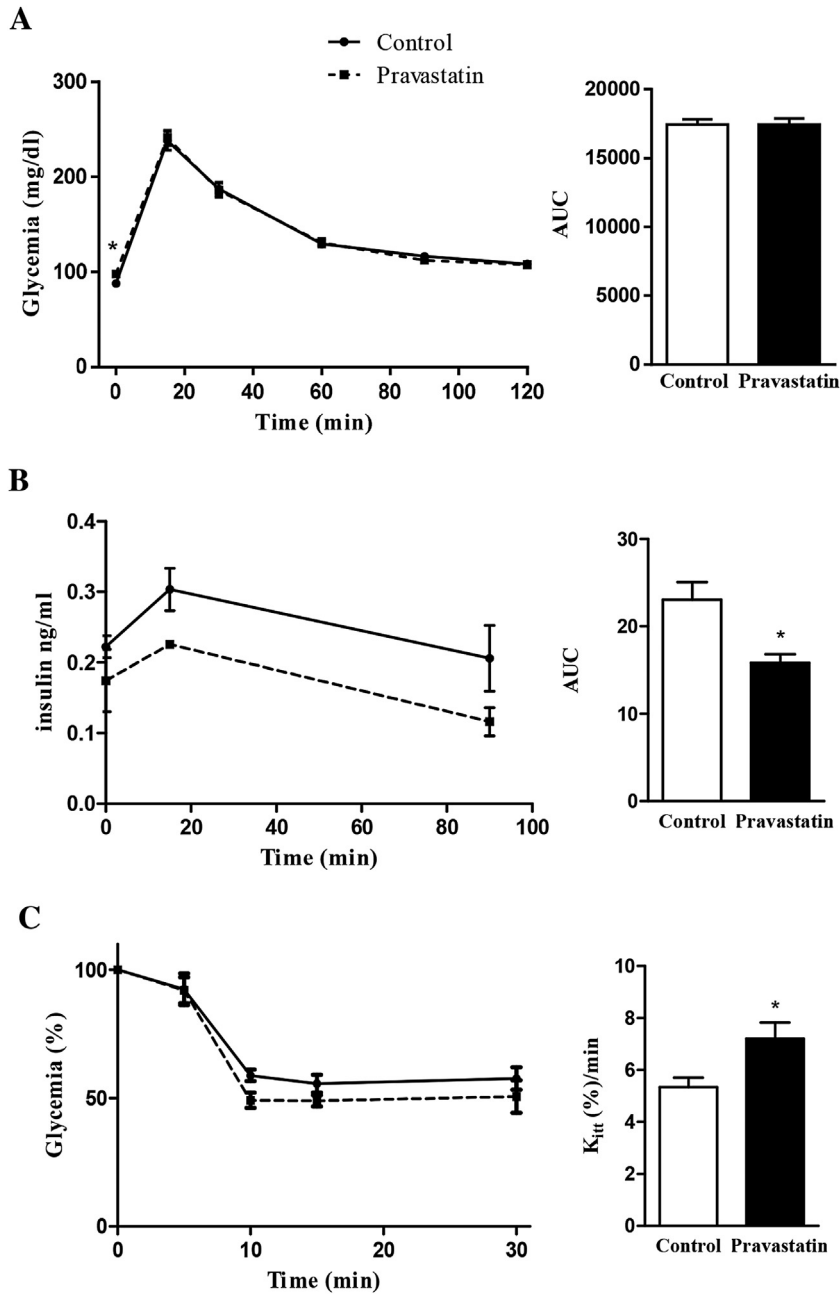$^*$ $p < 0.05$ Student $t$ test vs. respective control.

**Fig. 1.** Effect of two-month pravastatin treatment on glucose homeostasis in LDLr$^{-/-}$ mice.
Glucose (GTT) and insulin tolerance (ITT) tests were performed after 2 months of pravastatin treatment. (A) Blood glucose concentrations and areas under de curve (AUC) during the GTT ($n = 16$). (B) Plasma insulin concentrations and AUC during GTT ($n = 4$). C) Blood glucose concentrations and glucose disappearance rates (Kitt) during ITT ($n = 6$). Mean ± SE. $^*p < 0.05$.

channels and SNARE proteins are localized in cholesterol-rich domains called lipid rafts. Either deficiency or excess of membrane cholesterol can alter lipid raft composition and thus the exocytosis anchorage apparatus. Therefore, we analyzed the expression of the SNARE proteins synaptosomal-associated protein 25 KD (SNAP25) and Syntaxin 1A, which are present in plasma membrane lipid rafts, as well as the vesicle-associated membrane protein 2 (VAMP2) in isolated islets. Significant reductions in expression of these 3 SNARE proteins were observed in pravastatin-treated LDLr$^{-/-}$ mouse islets (35% for SNAP25, 30% for Syntaxin 1A, and 50% for VAMP2, Fig. 3A). Immunofluorescence was performed to confirm the relative expression and distribution of SNAREs in the islets (Fig. 3B). A marked reduction in Syntaxin-1A and VAMP2 abundance was observed in pravastatin-treated islets.

Furthermore, we observe β-cell membrane localization of Syntaxin 1A and a more diffuse (intracellular) pattern for VAMP2, which both are well co-localized with the insulin marker. In addition, we also analyzed whether the pravastatin-mediated reduction in islet cholesterol content modified glucose-stimulated Ca$^{+2}$ handling. As demonstrated in Fig. 3C, pravastatin-treated islets isolated from LDLr$^{-/-}$ mice had similar [Ca$^{+2}$] oscillatory behavior compared with non-treated control islets.

### 3.4. Two month pravastatin treatment induces cell death by apoptosis in pancreatic islets

We evaluated the possibility that pravastatin treatment of LDLr$^{-/-}$ mice could lead to cell death, and consequently reduce of
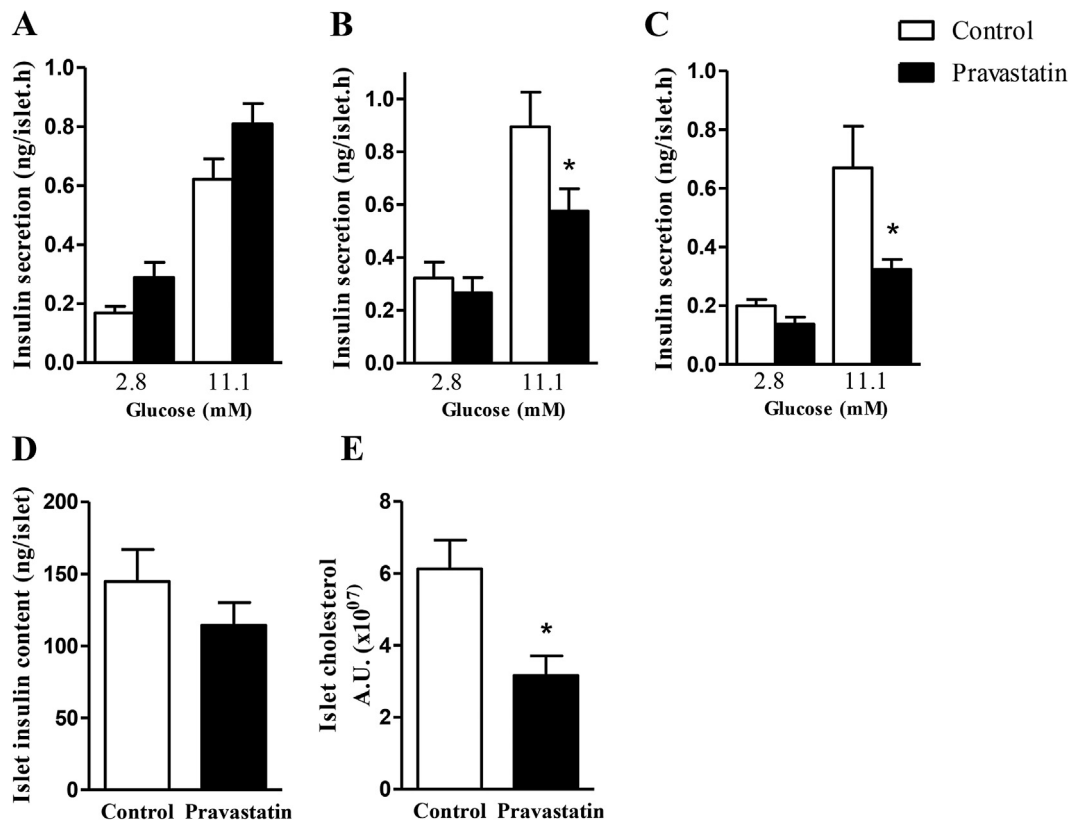
**Fig. 2.** Chronic pravastatin treatment reduces insulin secretion.
Insulin secretion from isolated islets from LDLr$^{-/-}$ mice in the presence of 2.8 mM and 11.1 mM glucose is represented after (A) one month ($n = 4$), (B) two months ($n = 8$) and (C) three months ($n = 4$) of pravastatin treatment. (D) Total insulin content in islets isolated from LDLr$^{-/-}$ mice after two months of treatment ($n = 4$). (E) Relative quantification of cholesterol in islets as detected by MALDI-MSI analysis. Mean ± SE *$p < 0.05$.

the number of insulin secreting cells. To investigate this pravastatin putative effect, we analyzed the expression of pro- and anti-apoptotic proteins Bax and Bcl2 and the protein levels of cleaved (activated) caspase-3, the final apoptotic effector caspase. Upon apoptotic stimuli, Bax, which is normally located in the cytoplasm, translocates to the mitochondrial membrane. Bax translocation initiates mitochondria-mediated apoptosis. Because Bcl-2 protein plays an anti-apoptotic role, we investigated whether pravastatin treatment would change the ratio of Bax/Bcl-2 in treated islets. As demonstrated in Fig. 4A, the Bax/Bcl-2 ratio was indeed increased in pravastatin-treated LDLr$^{-/-}$ mouse islets. In addition, increased cell apoptosis is indicated by 85% higher levels of cleaved caspase-3 in treated islets (Fig. 4A). Confirming these results, the number of apoptotic (TUNEL positive) cells was significantly increased after 2 months of pravastatin treatment (Fig. 4B). Finally, to assess cell metabolic activity, we measured NAD(P)H production in response to glucose stimulus. Thus, endogenous nucleotide fluorescence was followed along time after glucose (11.1 mM) stimulation and demonstrated a marked reduction in islets from pravastatin-treated mice (Fig. 4C). These results may represent a decrease in cell viability (number of cells) in the islets of pravastatin treated mice.

In contrast to islets, hepatocytes seem to not undergo pravastatin treatment-induced apoptosis because cleaved caspase-3 expression is not altered in treated and untreated mice livers (Supplementary Fig. 1).

### 3.5. Distinct pancreatic islets lipid markers after two months of pravastatin treatment

Using MALDI-MSI, a survey scan spectra of isolated untreated or pravastatin-treated islets were compared. Differences in the lipid profile were visible in fingerprinting analysis (data not shown), and statistical analysis (PCA) confirmed that both groups were clearly separated with an accuracy of 98% (Supplementary Fig. 3). For chemical marker identification, MS/MS reactions were performed and compared to the characteristic fragmentations that were observed in the Lipid MAPS database and also with software predictions. The chemical markers identified in pancreatic islets and the precursor ion fragmentation is demonstrated in Table 3. They consist mainly of phospholipids, tri- and diacylglycerol species and lactosyl-ceramides. The latter is recognized as a proapoptotic lipid molecule. Interestingly, most chemical markers of the pravastatin-treated group were oxidized lipids. Images of selected individual chemical markers distribution in mouse islets (Supplementary Fig. 4) show marked differences between groups.

### 3.6. Pravastatin induces cell death and oxidative stress (H$_2$O$_2$ production) in INS-1E cells

To confirm and expand in vivo and ex vivo data, we used insulin secreting INS-1E cells to verify pravastatin effects on the reactive oxygen (H$_2$O$_2$) production rates and apoptosis (indicated by cleaved caspase-3) (Fig. 5). Hydrogen peroxide net production is
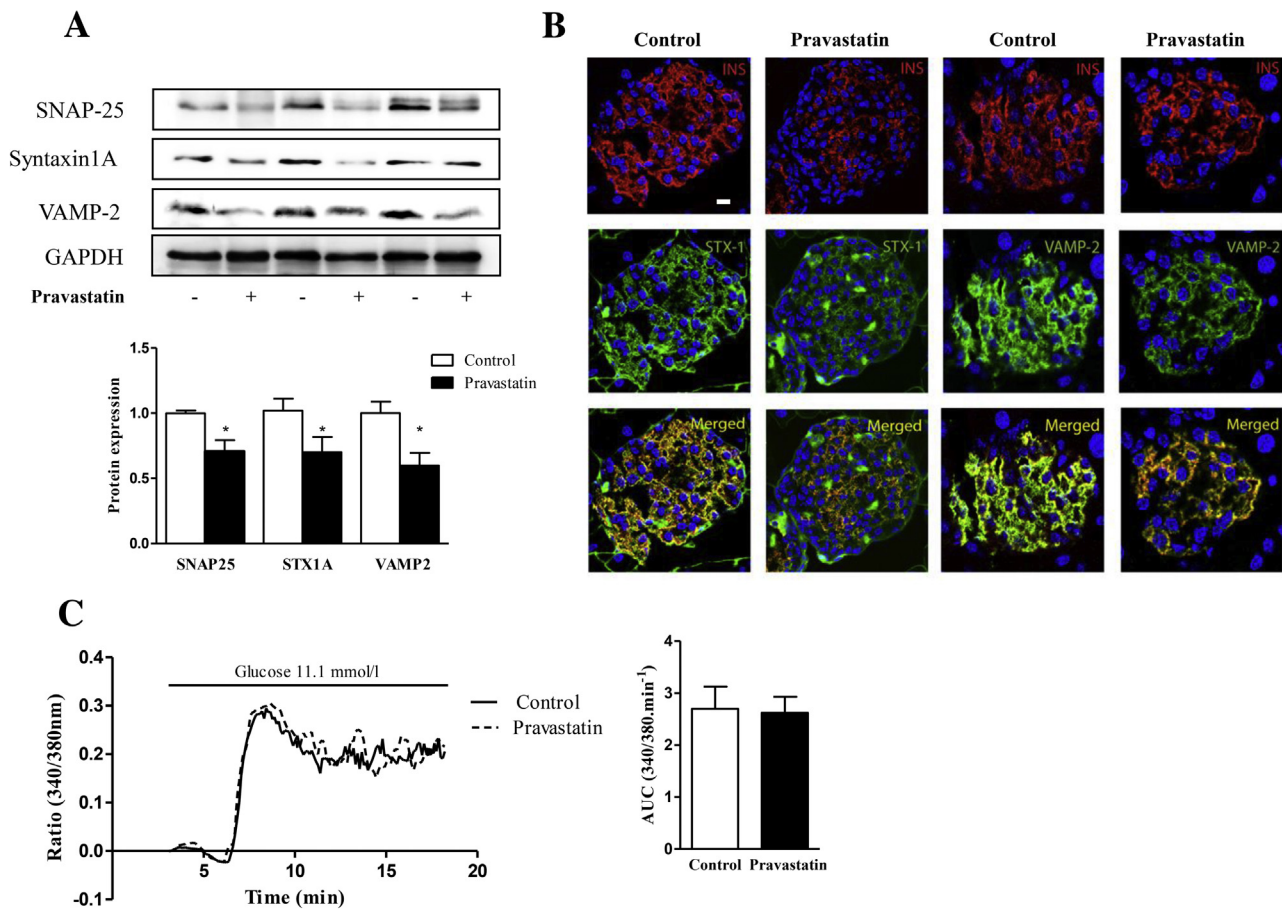
**A**



**B**



**C**



**Fig. 3.** Two-month pravastatin treatment decreases the expression of SNARE proteins but does not modulate intracellular calcium handling in isolated islets from LDLr$^{-/-}$ mice.
(A) Western blot analyses of SNARE proteins ($n = 5$) and (B) immunofluorescence staining of insulin and SNARE proteins Syntaxin 1A and VAMP2; Images are representative of $n = 3$ mice. Scale bar, 50 μm. (C) Representative curves and areas under the curve (AUC) of intracellular Ca$^{2+}$ oscillations in response to 11.1 mM glucose ($n = 7$). Mean ± SE $^*p < 0.05$.

significantly increased from 12 h incubation time and from 10 μM pravastatin dose (Fig. 5A and B). Specificity of this assay is demonstrated by catalase inhibition of fluorescence along time. Regarding cell death, the levels of the active effector caspase-3 were clearly demonstrated to be dependent on the incubation time and pravastatin dose (Fig. 5C). It is interesting that H$_2$O$_2$ production rates under 50 μM dose is always slightly lower than 10 μM pravastatin dose. This is probably a result of increased cell death at this dose, since activation of caspase 3 (Fig. 5C) is higher at 50 μM pravastatin dose.

## 4. Discussion

In the present study, contrary to the original hypothesis, we demonstrated that pravastatin treatment (for at least two months) of a hypercholesterolemic model (female LDLr$^{-/-}$ mice) disturbed glucose homeostasis (higher plasma levels in fasting and fed state) and resulted in marked reductions of fed insulinemia and ex vivo glucose-stimulated insulin secretion by isolated pancreatic islets. The mechanisms responsible for the latter effect are related to (1) reduction in protein levels of the SNARE proteins Syntaxin-1A, SNAP25 and VAMP-2 and (2) increased apoptosis signaling (Bax/Bcl2 ratio) and cell death (caspase-3 activation and Tunel positive cells). Additionally, by lipidomic analyses, we observed that pravastatin treatment increased lipid oxidative damage and the

content of lactosyl-ceramide, both findings may be related to cell death. Accordingly, we found that in vitro pravastatin induced time and dose dependent cell death and net production of H$_2$O$_2$ in insulin secreting INS-1 cells. Together, these results suggest that prolonged pravastatin treatment impairs the function of the exocytosis machinery and increases β-cell death probably as a consequence of a beta cell oxidative stress. These events may increase the risk of developing diabetes, as reported recently in several studies with statin treated patients.

Since the 90s, statin use has increased dramatically because of its great success in cardiovascular disease treatment, as it has reduced mortality rates by at least one third (Kashyap et al., 2003). However, recent studies have demonstrated that statins may be associated with an increased risk of developing type 2 diabetes (Cederberg et al., 2015; Sattar and Taskinen, 2012). While an early trial (WOSCOPS, the West of Scotland Coronary Prevention Study) (Freeman et al., 2001) suggested possible protection against diabetes, the JUPITER study (Justification for the Use of Statins in Prevention: An Intervention Trial Evaluating Rosuvastatin) (Ridker et al., 2008) documented an overall 25% increase in diabetes risk with statin treatment. A previous meta-analysis supports the concept that statins are indeed diabetogenic (Preiss et al., 2011) with varying effects depending on the dose, statin type, sex and pre-existing conditions. Sex stratification in the JUPITER study revealed that the diabetes risk was increased by 49% in women and
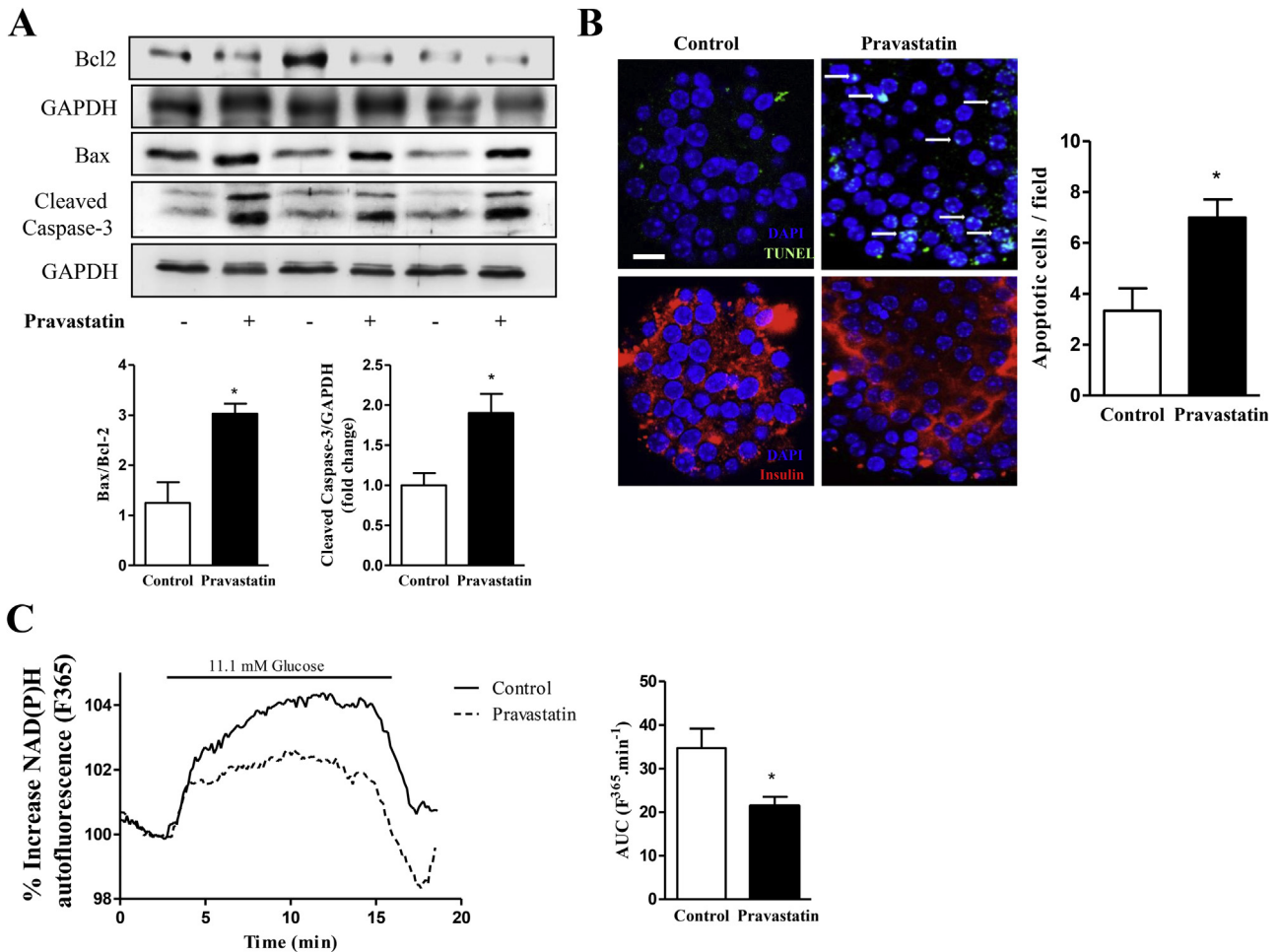
**A**



**B**



**C**



**Fig. 4.** Two-month pravastatin treatment impairs cell viability of islets from LDLr$^{-/-}$ mice.
(A) Expression (Western blot) of Bax, Bcl-2 and cleaved caspase-3 ($n = 5$). (B) Pancreatic islets were dispersed onto coverslips and stained for nicked DNA using TUNEL (green) and counter stained with insulin (red) and DAPI (blue). Scale bar, 50 μm. (Arrow: apoptotic cells); Images are representative of $n = 3$ mice. (C) Glucose (11.1 mM)-induced NAD (P)H production in isolated islets ($n = 5$). Mean ± SE *$p < 0.05$. (For interpretation of the references to color in this figure legend, the reader is referred to the web version of this article.)

**Table 3**

Most probable assignment based on mass to charge ratio ($m/z$) measurements of lipids detected by MALDI analysis of islets from LDLr$^{-/-}$ mice treated or not with pravastatin.

| Control | Lipid | [M−H]$^-$ | MS/MS | LMID |
|---|---|---|---|---|
| | PC (22:2/0:0) + O$_2$ | 606 | 562, 560 | LMGP01050135 |
| | PC (15:0/22:1) + O | 817 | 773, 671, 730 | LMGP01011427 |
| | PI (18:3/0:0) + O | 609 | 565, 591 | LMGP06050016 |
| | PE (17:1/22:4) | 779 | 590, 546, 735 | LMGP02010589 |
| | PE (18:2/22:2) | 795 | 751, 769 | LMGP02010677 |
| | PS (15:0/22:2) | 801 | 757, 775 | LMGP03010158 |
| | PA (13:0/18:2) | 629 | 585 | LMGP10010076 |
| Pravastatin | Lipid | [M−H]$^-$ | MS/MS | LMID |
| | PS (22:6/0:0) + O$_2$ | 600 | 556 | LMGP03050013 |
| | TG (18:3/18:3/ 20:1) + O$_3$H | 952 | 908 | LMGL03010722 |
| | PG (12:0/19:1) + O | 721 | 677, 577 | LMGP04010058 |
| | PE (16:0/20:5) + O | 739 | 494 | LMGP02020095 |
| | DG (20:4/20:5/0:0) + O | 677 | 633, 651 | LMGL02010217 |
| | PE (16:0/20:4) + O | 741 | 654 | LMGP02020019 |
| | LacCer (18:1/24:0) | 973 | 947, 833 | LMSP0501AB07 |

PC, phosphatidylcholine; PE, phosphatidylethanolamine; PI, phosphatidylinositol; PS, phosphatidylserine; PA, phosphatidic acid; TG, triacylglycerol; PG, phosphoglycerol; DG, diacylglycerol; LacCer, Lactosyl-ceramide ($n = 4$). [M−H]$^-$ deprotonated molecular ions. LMID, lipid map database identification.

by only 14% in men (Mora et al., 2010). Goodarzi et al. reported a significant relationship ($p = 0.036$) between the percent of women in the statin trials and the odds ratio for diabetes (Goodarzi et al., 2013). The only trial (WOSCOPS) that suggested reduced diabetes in statin-treated subjects consisted of only men. In addition, statin use among postmenopausal women in the Women's Health Initiative was associated with an increased risk of type 2 diabetes. This effect was observed for all types of statins and appeared to be a class effect (Culver et al., 2012). The greater risk of statin-induced diabetes in women may have been noticed only recently because they are under-represented in most statin trials.

During the process of cholesterol synthesis from acetyl CoA, various metabolites such as isoprenoids, farnesylpyrophosphate, geranylgeranyl pyrophosphate and coenzyme Q10 (CoQ10) are normally produced. By inhibiting HMG-CoA reductase, statins also inhibit the production of these metabolites that may affect insulin secretion or insulin sensitivity (Brault et al., 2014). For example, CoQ10 is an essential part of the mitochondrial respiratory chain; hence, it is necessary for ATP production and also functions as an antioxidant. Several statins reduce the circulating levels of CoQ10 (Folkers et al., 1990; Rundek et al., 2004). Incubation of permeabilized rat soleus muscle fiber biopsies with increasing simvastatin concentrations resulted in diminished mitochondrial respiration rates, increased H$_2$O$_2$ and lactate release and decreased
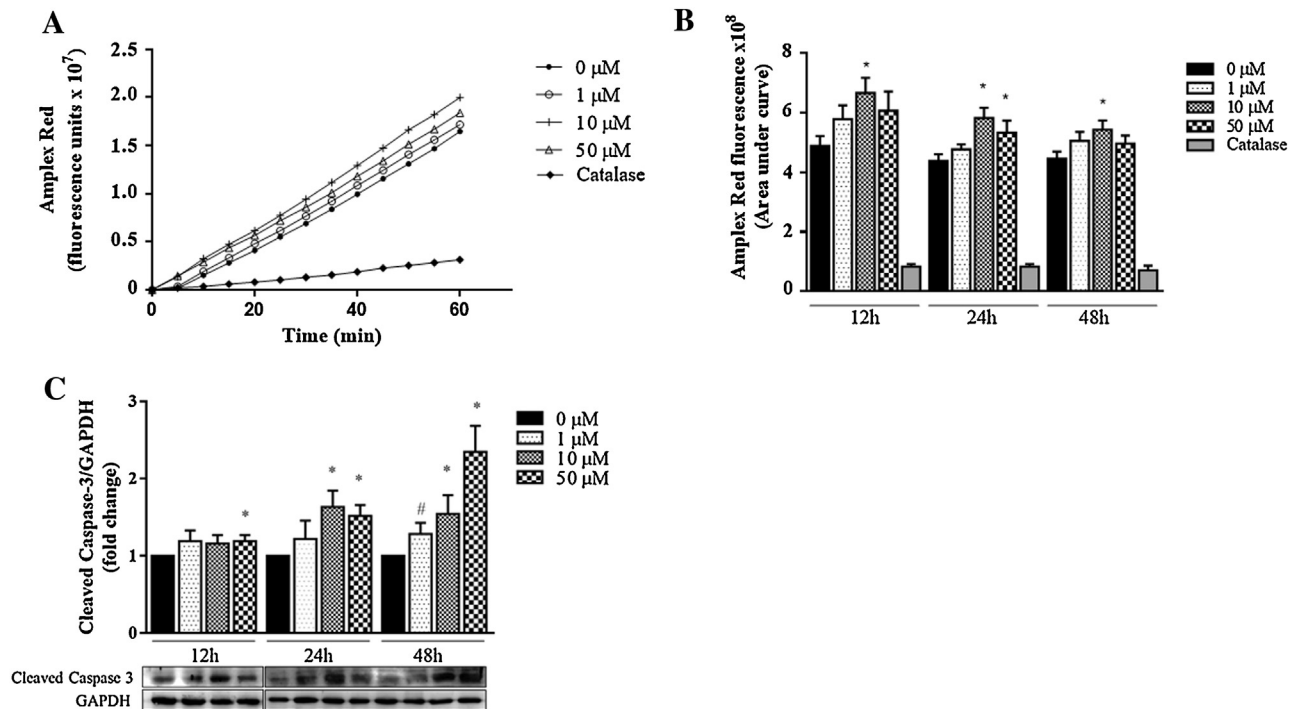
**Fig. 5.** Pravastatin increases $H_2O_2$ production and caspase-3 activation in treated INS1E cells.
$H_2O_2$ generation in INS1E cells treated with pravastatin was determined by the Amplex red probe. (A) Representative fluorescence curve after 24 h treatment with increasing doses of pravastatin. (B) Area under the curves of Amplex Red induced fluorescence after treatment with increasing doses of pravastatin (0, 1, 10, 50 μM) for increasing periods of incubation (12, 24 and 48 h). C) Amount of cleaved Caspase 3 (Western blot analyses) in INS1E cells treated with pravastatin for the indicated times. Four independent experiment performed ($n = 4$). Values are Mean ± SE. $^*P < 0.05$ and $\#P = 0.058$ compared with control (Student's $t$ test).

CoQ10 content. Additions of mevalonate, CoQ10 or L-carnitine abolished the effects of statins but only mevalonate prevented the decrease in CoQ10 content (La Guardia et al., 2013). These findings reveal that statins decrease CoQ10 synthesis in situ, and that CoQ10 plays key roles in mitochondrial phosphorylating respiration and as an antioxidant.

A recent study by Zuniga-Hertz et al. (2015) reported that the blockade of cholesterol biosynthesis by simvastatin in insulin secreting INS-1E cells resulted in the reductions of isoprenoids, total cholesterol content and glucose stimulated insulin secretion. The decrease in insulin secretion was prevented by cell loading with the isoprenyl molecule geranylgeranyl pyrophosphate.

A study from Bellia et al. followed T2D subjects that had been treated with rosuvastatin or simvastatin for six months and observed deterioration of glycemic control without changes in insulin sensitivity, suggesting that deterioration of insulin secretion is probably the diabetogenic mechanism of statins (Bellia et al., 2012). A systematic review and meta-analysis of patients without diabetes receiving different statins reported that pravastatin improved insulin sensitivity while simvastatin worsened it (Baker et al., 2010). It has been hypothesized that lipophilic statins might be more diabetogenic than hydrophilic statins (e.g., pravastatin) (Schachter, 2005). The effect of statins on insulin sensitivity is a matter that is widely debated, and there seems to be no "class effect".

In this work, we observed that most lipid biomarkers in the pravastatin-treated mouse pancreatic islets were oxidized. Pancreatic islets have low activity of free radical detoxifying enzymes such as catalase, superoxide dismutase (SOD) and glutathione peroxidase compared with other tissues such as liver or kidney; thus, islets are more sensitive to damage caused by oxidative stress (Acharya and Ghaskadbi, 2010). Therefore, our

findings suggest that the oxidative stress (indicated by the presence of oxidized lipids in islet and by INS-1 cell $H_2O_2$ production) plays a key role in islet deterioration in terms of its viability (apoptosis) and functionality during pravastatin treatment, which is not observed in other tissues such as liver. Consistent with this view, it was previously demonstrated that SNARE proteins are targets of reactive oxygen species, and once oxidized, they compromise the vesicle fusion mechanism (Giniatullin et al., 2006).

Lactosyl-ceramide (LacCer) has been recognized as a second messenger in mediating diverse cellular events including cell proliferation (Bhunia et al., 1996) but also programmed cell death (Martin et al., 2006). LacCer can generate superoxide via NAD(P)H oxidase activation (Bhunia et al., 1997). We detected this apoptotic agent as a biomarker in islets from pravastatin-treated mice. This result is in accordance with other apoptotic indicators including an increase in the Bax/Bcl-2 ratio, activated caspase-3, Tunel positive cells and reduced glucose stimulated NADPH production. Velho et al. (2006) demonstrated that statins act directly on liver mitochondria either in vivo or in vitro to induce permeability transition, which is a process involved in cell death. The authors demonstrated that this effect was dose- and statin type-dependent and was mediated by the decrease in mitochondrial membrane protein thiol groups.

In conclusion, the present findings together with previous reported evidences support the proposal that the toxic effects of pravastatin may be caused by the decrease in the biosynthesis of intermediate metabolites such as CoQ10 and increased ROS generation, which in turn triggers cell death and impairs insulin secretion. Our results reveal new cellular and molecular mechanisms that may explain the increased onset of diabetes in statin-treated subjects.

## Conflict of interest

None.

## Acknowledgements

## Appendix A. Supplementary data

Supplementary data associated with this article can be found, in the online version, at http://dx.doi.org/10.1016/j.tox.2015.12.007.

## References

Acharya, J.D., Ghaskadbi, S.S., 2010. Islets and their antioxidant defense. Islets 2, 225–235.

Baker, W.L., Talati, R., White, C.M., Coleman, C.I., 2010. Differing effect of statins on insulin sensitivity in non-diabetics: a systematic review and meta-analysis. Diabetes Res. Clin. Pract. 87, 98–107.

Bellia, A., Rizza, S., Lombardo, M.F., Donadel, G., Fabiano, R., Andreadi, K., Quon, M.J., Sbraccia, P., Federici, M., Tesauro, M., Cardillo, C., Lauro, D., 2012. Deterioration of glucose homeostasis in type 2 diabetic patients one year after beginning of statins therapy. Atherosclerosis 223, 197–203.

Bhunia, A.K., Han, H., Snowden, A., Chatterjee, S., 1996. Lactosylceramide stimulates Ras-GTP loading, kinases (MEK, Raf), p44 mitogen-activated protein kinase, and c-fos expression in human aortic smooth muscle cells. J. Biol. Chem. 271, 10660–10666.

Bhunia, A.K., Han, H., Snowden, A., Chatterjee, S., 1997. Redox-regulated signaling by lactosylceramide in the proliferation of human aortic smooth muscle cells. J. Biol. Chem. 272, 15642–15649.

Bonfleur, M.L., Ribeiro, R.A., Balbo, S.L., Vanzela, E.C., Carneiro, E.M., de Oliveira, H.C., Boschero, A.C., 2011. Lower expression of PKAalpha impairs insulin secretion in islets isolated from low-density lipoprotein receptor (LDLR(−/−)) knockout mice. Metabolism 60, 1158–1164.

Bonfleur, M.L., Vanzela, E.C., Ribeiro, R.A., de Gabriel Dorighello, G., de Franca Carvalho, C.P., Collares-Buzato, C.B., Carneiro, E.M., Boschero, A.C., de Oliveira, H. C., 2010. Primary hypercholesterolaemia impairs glucose homeostasis and insulin secretion in low-density lipoprotein receptor knockout mice independently of high-fat diet and obesity. Biochim. Biophys. Acta 1801, 183–190.

Boschero, A.C., Delattre, E., 1985. The mechanism of gentamicin-inhibited insulin release by isolated islets. Arch. Int. Pharmacodyn. Ther. 273, 167–176.

Brault, M., Ray, J., Gomez, Y.H., Mantzoros, C.S., Daskalopoulou, S.S., 2014. Statin treatment and new-onset diabetes: a review of proposed mechanisms. Metabolism 63, 735–745.

Brunham, L.R., Kruit, J.K., Pape, T.D., Timmins, J.M., Reuwer, A.Q., Vasanji, Z., Marsh, B.J., Rodrigues, B., Johnson, J.D., Parks, J.S., Verchere, C.B., Hayden, M.R., 2007. Beta-cell ABCA1 influences insulin secretion: glucose homeostasis and response to thiazolidinedione treatment. Nat. Med. 13, 340–347.

Bruns, D., Jahn, R., 2002. Molecular determinants of exocytosis. Pflugers Arch. 443, 333–338.

Cederberg, H., Stancakova, A., Yaluri, N., Modi, S., Kuusisto, J., Laakso, M., 2015. Increased risk of diabetes with statin treatment is associated with impaired insulin sensitivity and insulin secretion: a 6 year follow-up study of the METSIM cohort. Diabetologia 58, 1109–1117.

Chamberlain, L.H., Burgoyne, R.D., Gould, G.W., 2001. SNARE proteins are highly enriched in lipid rafts in PC12 cells: implications for the spatial control of exocytosis. Proc. Natl. Acad. Sci. U. S. A. 98, 5619–5624.

Culver, A.L., Ockene, I.S., Balasubramanian, R., Olendzki, B.C., Sepavich, D.M., Wactawski-Wende, J., Manson, J.E., Qiao, Y., Liu, S., Merriam, P.A., Rahilly-Tierny, C., Thomas, F., Berger, J.S., Ockene, J.K., Curb, J.D., Ma, Y., 2012. Statin use and risk of diabetes mellitus in postmenopausal women in the Women's Health Initiative. Arch. Intern. Med. 172, 144–152.

Davignon, J., Jacob, R.F., Mason, R.P., 2004. The antioxidant effects of statins. Coron. Artery Dis. 15, 251–258.

Desai, C.S., Martin, S.S., Blumenthal, R.S., 2014. Non-cardiovascular effects associated with statins. BMJ 349, g3743.

Folkers, K., Langsjoen, P., Willis, R., Richardson, P., Xia, L.J., Ye, C.Q., Tamagawa, H., 1990. Lovastatin decreases coenzyme Q levels in humans. Proc. Natl. Acad. Sci. U. S. A. 87, 8931–8934.

Freeman, D.J., Norrie, J., Sattar, N., Neely, R.D., Cobbe, S.M., Ford, I., Isles, C., Lorimer, A.R., Macfarlane, P.W., McKillop, J.H., Packard, C.J., Shepherd, J., Gaw, A., 2001. Pravastatin and the development of diabetes mellitus: evidence for a protective treatment effect in the West of Scotland Coronary Prevention Study. Circulation 103, 357–362.

Fryirs, M., Barter, P.J., Rye, K.A., 2009. Cholesterol metabolism and pancreatic beta-cell function. Curr. Opin. Lipidol. 20, 159–164.

Giniatullin, A.R., Darios, F., Shakirzyanova, A., Davletov, B., Giniatullin, R., 2006. SNAP25 is a pre-synaptic target for the depressant action of reactive oxygen species on transmitter release. J. Neurochem. 98, 1789–1797.

Gleason, C.E., Gonzalez, M., Harmon, J.S., Robertson, R.P., 2000. Determinants of glucose toxicity and its reversibility in the pancreatic islet beta-cell line: HIT-T15. Am. J. Physiol. Endocrinol. Metab. 279, E997–1002.

Goodarzi, M.O., Li, X., Krauss, R.M., Rotter, J.I., Chen, Y.D., 2013. Relationship of sex to diabetes risk in statin trials. Diabetes Care 36, e100–101.

Halban, P.A., Polonsky, K.S., Bowden, D.W., Hawkins, M.A., Ling, C., Mather, K.J., Powers, A.C., Rhodes, C.J., Sussel, L., Weir, G.C., 2014. Beta-cell failure in type 2 diabetes: postulated mechanisms and prospects for prevention and treatment. J. Clin. Endocrinol. Metab. 99, 1983–1992.

Hanson, P.I., Heuser, J.E., Jahn, R., 1997. Neurotransmitter release—four years of SNARE complexes. Curr. Opin. Neurobiol. 7, 310–315.

Hao, M., Head, W.S., Gunawardana, S.C., Hasty, A.H., Piston, D.W., 2007. Direct effect of cholesterol on insulin secretion: a novel mechanism for pancreatic beta-cell dysfunction. Diabetes 56, 2328–2338.

Ishikawa, M., Iwasaki, Y., Yatoh, S., Kato, T., Kumadaki, S., Inoue, N., Yamamoto, T., Matsuzaka, T., Nakagawa, Y., Yahagi, N., Kobayashi, K., Takahashi, A., Yamada, N., Shimano, H., 2008. Cholesterol accumulation and diabetes in pancreatic beta-cell-specific SREBP-2 transgenic mice: a new model for lipotoxicity. J. Lipid Res. 49, 2524–2534.

Kashyap, M.L., Tavintharan, S., Kamanna, V.S., 2003. Optimal therapy of low levels of high density lipoprotein-cholesterol. Am. J. Cardiovasc. Drugs 3, 53–65.

La Guardia, P.G., Alberici, L.C., Ravagnani, F.G., Catharino, R.R., Vercesi, A.E., 2013. Protection of rat skeletal muscle fibers by either L-carnitine or coenzyme Q10 against statins toxicity mediated by mitochondrial reactive oxygen generation. Front. Physiol. 4, 103.

Martin, S.F., Williams, N., Chatterjee, S., 2006. Lactosylceramide is required in apoptosis induced by N-Smase. Glycoconjugate J. 23, 147–157.

Mora, S., Glynn, R.J., Hsia, J., MacFadyen, J.G., Genest, J., Ridker, P.M., 2010. Statins for the primary prevention of cardiovascular events in women with elevated high-sensitivity C-reactive protein or dyslipidemia: results from the Justification for the Use of Statins in Prevention: an Intervention Trial Evaluating Rosuvastatin (JUPITER) and meta-analysis of women from primary prevention trials. Circulation 121, 1069–1077.

Poitout, V., Robertson, R.P., 2008. Glucolipotoxicity: fuel excess and beta-cell dysfunction. Endocr. Rev. 29, 351–366.

Preiss, D., Seshasai, S.R., Welsh, P., Murphy, S.A., Ho, J.E., Waters, D.D., DeMicco, D.A., Barter, P., Cannon, C.P., Sabatine, M.S., Braunwald, E., Kastelein, J.J., de Lemos, J.A., Blazing, M.A., Pedersen, T.R., Tikkanen, M.J., Sattar, N., Ray, K.K., 2011. Risk of incident diabetes with intensive-dose compared with moderate-dose statin therapy: a meta-analysis. JAMA 305, 2556–2564.

Rafacho, A., Marroquí, L., Taboga, S.R., 2010. Glucocorticoids in vivo induce both insulin hypersecretion and enhanced glucose sensitivity of stimulus-secretion coupling in isolated rat islets. Endocrinology 151, 85–95.

Ridker, P.M., Danielson, E., Fonseca, F.A., Genest, J., Gotto Jr., A.M., Kastelein, J.J., Koenig, W., Libby, P., Lorenzatti, A.J., MacFadyen, J.G., Nordestgaard, B.G., Shepherd, J., Willerson, J.T., Glynn, R.J., Group, J.S., 2008. Rosuvastatin to prevent vascular events in men and women with elevated C-reactive protein. N. Engl. J. Med. 359, 2195–2207.

Rundek, T., Naini, A., Sacco, R., Coates, K., DiMauro, S., 2004. Atorvastatin decreases the coenzyme Q10 level in the blood of patients at risk for cardiovascular disease and stroke. Arch. Neurol. 61, 889–892.

Sattar, N., Taskinen, M.R., 2012. Statins are diabetogenic—myth or reality? Atherosclerosis Suppl. 13, 1–10.

Schachter, M., 2005. Chemical: pharmacokinetic and pharmacodynamic properties of statins: an update. Fundam. Clin. Pharm. 19, 117–125.

Scott, A.M., Atwater, I., Rojas, E., 1981. A method for the simultaneous measurement of insulin release and B cell membrane potential in single mouse islets of Langerhans. Diabetologia 21, 470–475.

Souza, J.C., Vanzela, E.C., Ribeiro, R.A., Rezende, L.F., de Oliveira, C.A., Carneiro, E.M., Oliveira, H.C., Boschero, A.C., 2013. Cholesterol reduction ameliorates glucose-induced calcium handling and insulin secretion in islets from low-density lipoprotein receptor knockout mice. Biochim. Biophys. Acta 1831, 769–775.

Taverna, E., Saba, E., Rowe, J., Francolini, M., Clementi, F., Rosa, P., 2004. Role of lipid microdomains in P/Q-type calcium channel (Cav2: 1) clustering and function in presynaptic membranes. J. Biol. Chem. 279, 5127–5134.

Taylor, F., Huffman, M.D., Macedo, A.F., Moore, T.H., Burke, M., Davey Smith, G., Ward, K., Ebrahim, S., 2013. Statins for the primary prevention of cardiovascular disease. Cochrane Database Syst. Rev. 1, CD004816.

Unger, R.H., 1995. Lipotoxicity in the pathogenesis of obesity-dependent NIDDM: genetic and clinical implications. Diabetes 44, 863–870.

Urayama, S., Zou, W., Brooks, K., Tolstikov, V., 2010. Comprehensive mass spectrometry based metabolic profiling of blood plasma reveals potent discriminatory classifiers of pancreatic cancer. Rapid Commun. Mass Spectrom. 24, 613–620.

Velho, J.A., Okanobo, H., Degasperi, G.R., Matsumoto, M.Y., Alberici, L.C., Cosso, R.G., Oliveira, H.C., Vercesi, A.E., 2006. Statins induce calcium-dependent mitochondrial permeability transition. Toxicology 219, 124–132.

Vikman, J., Jimenez-Feltstrom, J., Nyman, P., Thelin, J., Eliasson, L., 2009. Insulin secretion is highly sensitive to desorption of plasma membrane cholesterol. FASEB J. 23, 58–67.

Wiser, O., Trus, M., Hernandez, A., Renstrom, E., Barg, S., Rorsman, P., Atlas, D., 1999. The voltage sensitive Lc-type $Ca^{2+}$ channel is functionally coupled to the exocytotic machinery. Proc. Natl. Acad. Sci. U. S. A. 96, 248–253.

Zuniga-Hertz, J.P., Rebelato, E., Kassan, A., Khalifa, A.M., Ali, S.S., Patel, H.H., Abdulkader, F., 2015. Distinct pathways of cholesterol biosynthesis impact on insulin secretion. J. Endocrinol. 224 (January (1)), 75–84. doi:http://dx.doi.org/10.1530/JOE-14-0348.